

# Altered coordination between frontal delta and parietal alpha networks underlies anhedonia and depressive rumination in major depressive disorder

Zenas C. Chao, PhD; Daniel G. Dillon, PhD; Yi-Hung Liu, PhD;  
Elyssa M. Barrick, BA, BS; Chien-Te Wu, PhD

**Background:** A hyperactive default mode network (DMN) has been observed in people with major depressive disorder (MDD), and weak DMN suppression has been linked to depressive symptoms. However, whether dysregulation of the DMN contributes to blunted positive emotional experience in people with MDD is unclear. **Methods:** We recorded 128-channel electroencephalograms (EEGs) from 24 participants with MDD and 31 healthy controls in a resting state (RS) and an emotion-induction state (ES), in which participants engaged with emotionally positive pictures. We combined Granger causality analysis and data-driven decomposition to extract latent brain networks shared among states and groups, and we further evaluated their interactions across individuals. **Results:** We extracted 2 subnetworks. Subnetwork 1 represented a delta ( $\delta$ )-band (1–4 Hz) frontal network that was activated more in the ES than the RS (i.e., task-positive). Subnetwork 2 represented an alpha ( $\alpha$ )-band (8–13 Hz) parietal network that was suppressed more in the ES than the RS (i.e., task-negative). These subnetworks were anticorrelated in both the healthy control and MDD groups, but with different sensitivities: for participants with MDD to achieve the same level of task-positive (subnetwork 1) activation as healthy controls, more suppression of task-negative (subnetwork 2) activation was necessary. Furthermore, the anticorrelation strength in participants with MDD correlated with the severity of 2 core MDD symptoms: anhedonia and rumination. **Limitations:** The sample size was small. **Conclusion:** Our findings revealed altered coordination between 2 functional networks in MDD and suggest that weak suppression of the task-negative  $\alpha$ -band parietal network contributes to blunted positive emotional responses in adults with depression. The subnetworks identified here could be used for diagnosis or targeted for treatment in the future.

## Introduction

Major depressive disorder (MDD) is characterized by a wide range of symptoms, including persistent and profound sadness, lack of mood reactivity, repetitive and passive thinking loops (depressive rumination), and reduced ability to feel pleasure (anhedonia).<sup>1</sup> A leading cause of disability worldwide, MDD has become even more prevalent as a result of the COVID-19 pandemic.<sup>2</sup> New insights into the etiology and treatment of MDD are greatly needed, but the heterogeneity of the disorder presents a challenge.

Several neurobiological mechanisms have been related to the etiology of MDD,<sup>3–8</sup> but one promising hypothesis proposes that dysregulation of the default mode network (DMN) plays a causal role in MDD.<sup>5,6,9,10</sup> This hypothesis is appealing because abnormalities in the DMN could contribute directly to rumination in adults with depression,<sup>11</sup> which could in

turn lead to other symptoms. For instance, the excessive self-directed negative thinking that characterizes rumination could make it difficult for adults with depression to engage with positive stimuli in their environment, contributing to anhedonia. In this way, the DMN dysregulation hypothesis could help explain why MDD is characterized by a wide variety of symptoms. To advance this idea, the current analysis focused on testing the DMN dysregulation hypothesis and relating it to emotional responses in adults with MDD.

The DMN dysregulation hypothesis is supported by many neuroimaging studies. First, higher activation, stronger functional connectivity or both are often observed in the DMN during the resting state in people with MDD compared to healthy controls.<sup>5,10,12</sup> Second, people with MDD have shown reduced resting-state functional connectivity between the medial prefrontal cortex (part of the DMN) and the affective network (likely associated with their depressive rumination),<sup>10</sup>

**Correspondence to:** Z.C. Chao and C. Wu, International Research Center for Neurointelligence (WPI-IRCN), UTIAS, The University of Tokyo, Tokyo, 113-0033, Japan; zenas.c.chao@gmail.com, chientevincewu@gmail.com

Submitted Mar. 11, 2022; Revised Apr. 3, 2022; Revised Jul. 25, 2022; Revised Aug. 18, 2022; Accepted Aug. 27, 2022

**Cite as:** *J Psychiatry Neurosci* 2022 November 1;47(6). doi: 10.1503/jpn.220046

or increased resting-state functional connectivity between the DMN and the subgenual prefrontal or cingulate cortex.<sup>9,11,13</sup> Third, multimodal neuroimaging studies have found that resting-state  $\delta$ -band (~1–4 Hz) electroencephalogram (EEG) activities in the prefrontal region correlate with functional MRI (fMRI) activations in the DMN,<sup>14</sup> and such activities positively correlate with symptom severity in MDD.<sup>15,16</sup> Some studies suggest that DMN dysregulation occurs only in some subtypes of MDD, such as the depressed-mood and anhedonic subtypes.<sup>17–19</sup>

A limitation of this previous work is that the effect of depression on the function of the DMN has been widely tested while participants were resting quietly, but it remains unclear whether the DMN contributes to abnormal emotional responses in people with MDD. Treatment-oriented research is encouraging, because aspects of the DMN serve as targets for brain stimulation in MDD treatments,<sup>20</sup> and can help predict responses to antidepressant medications;<sup>21–25</sup> these 2 facts suggest that DMN dysfunction may play an important role in the abnormal emotional responses that characterize depression. Nevertheless, it is crucial to identify any direct links between DMN dysfunction and abnormal emotion in people with MDD for more effective treatment and diagnosis. Such links have been explored using tasks that require implicit processing of emotional stimuli, such as emotion identification and emotional Stroop tasks, where altered functional connectivity in the DMN — or between the DMN and other networks — has been found.<sup>26–29</sup> However, tasks that require explicit engagement with emotional stimuli are needed. Furthermore, most DMN studies used seed-based approaches based on predetermined anatomic regions.<sup>26–29</sup> Although this approach has been productive, it cannot provide a comprehensive view of the network interactions that may be affected by depression.

To examine comprehensive network interactions associated with abnormal emotion in people with MDD, we used an unbiased, data-driven approach to decompose EEG data from an emotion-induction task in which participants used mental imagery to engage with positive stimuli. We adopted positive stimuli because depression is associated with weak positive emotional responses<sup>30</sup> that have been linked to anhedonia (loss of pleasure), which predicts a longer and more severe course of MDD.<sup>31</sup> Decomposition analysis enabled the extraction of latent subnetworks with unique activity patterns and functional characteristics,<sup>32–34</sup> which allowed further evaluation of their interactions and contributions to depressive symptoms.

## Methods

### Participants

We included data from 24 participants with MDD and 31 healthy controls recruited from the community. All participants provided signed informed consent to a protocol approved by the Partners HealthCare Human Research Committee (Partners IRB #2014P001980) and were compensated US\$25 per hour. Participants were screened using the Beck Depression Inventory II;<sup>35</sup> potentially eligible participants were further interviewed and their diagnosis of MDD (or

lack thereof) was confirmed using the Mini-International Neuropsychiatric Interview, version 6.0,<sup>36</sup> on the EEG recording day. All screening and clinical interviews were performed by a trained clinical interviewer at McLean Hospital, Belmont, Massachusetts, United States.

Inclusion criteria for the MDD group were as follows: endorsed symptoms consistent with a current major depressive episode; score of 13 or higher on the Beck Depression Inventory II;<sup>35</sup> no other DSM-IV Axis I psychopathology with the exception of generalized anxiety, social anxiety or specific phobia (all of which are highly comorbid with MDD); no medication use in the previous 2 weeks (6 weeks for fluoxetine, 6 months for neuroleptics). Participants in the healthy control group had to report no current or past DSM-IV Axis I psychopathology. The present study used the same data as Wu and colleagues.<sup>37</sup>

### Procedures

We administered 2 resting-state and 2 emotion-induction sessions in alternating order, starting with a resting-state session and using the protocol in Liao and colleagues.<sup>38</sup> The protocol was programmed and controlled using PsychoPy<sup>39</sup> on a PC, and all stimuli were displayed on a 22-inch monitor.

For each resting-state trial (Appendix 1, Figure S1A, available at [www.jpn.ca/lookup/doi/10.1503/jpn.220046/tab-related-content](http://www.jpn.ca/lookup/doi/10.1503/jpn.220046/tab-related-content)), participants viewed a 5-second countdown before seeing a fixation cross for 54 seconds. During this time, participants were instructed to maintain fixation on the cross while relaxing — they were not asked to direct their thoughts in any way. Three trials were performed in each resting-state session.

For each emotion-induction trial (Appendix 1, Figure S1B), participants were asked to engage with positive pictures using mental imagery.<sup>40</sup> Again, each trial began with a 5-second countdown, after which a positive picture was displayed for 6 seconds. During this time, participants were instructed to imagine themselves, their significant others or their close friends experiencing the positive events depicted in each picture. After the picture disappeared, participants used Likert scales paired with the Self-Assessment Manikin<sup>41</sup> to rate the level of induced valence (1 = most unpleasant, 9 = most pleasant) and arousal (1 = calm, 9 = excited) in each trial. The pictures used in the study were selected from the International Affective Picture System,<sup>42</sup> and all were considered high-valence and high-arousal because they all had normative ratings greater than 5 for valence and arousal.

Each emotion-induction session included 27 trials and lasted about 7 minutes (range: 6–9 minutes), with some variability because the emotion ratings were self-paced. Each trial used a different picture. The subjective ratings elicited by this task have been reported in an earlier paper, which showed lower (i.e., less positive) induced valence in the MDD group than in the healthy control group,<sup>37</sup> suggesting blunted positive emotion in people with MDD.

After all 4 sessions were finished, participants completed the Beck Depression Inventory II,<sup>35</sup> the Mood and Anxiety Symptom Questionnaire (MASQ),<sup>43</sup> the Ruminative Responses Scale (RRS)<sup>44</sup> and the Pittsburgh Sleep Quality Index.<sup>45</sup> Details of the questionnaires are provided in Appendix 1.

### Data acquisition and analysis

The EEG data were recorded using a 128-sensor HydroCel GSN network and high impedance amplifier from Electrical Geodesics Inc (see Appendix 1 for details). For each participant, the data from the 2 emotion-induction sessions (ES) were segmented to obtain 54 trials of 6 seconds, and the data from the first resting-state session (RS) were segmented into 27 non-overlapping 6-second windows. We used only the first resting-state session in our analysis because the second resting-state session could have contained emotion-related activity from the first emotion-induction session. We applied further analyses to those 6-second segments (54 trials from the ES and 27 windows from the RS conditions; see data pre-processing, functional connectivity analysis, data-driven decomposition analysis and statistical tests in Appendix 1).

## Results

To acquire robust functional connectivity measures,<sup>46</sup> we estimated the reference-free current source density from 128-channel EEG signals in 24 participants with MDD and 31 healthy controls during the RS and ES conditions (demographic details in Table 1), and measured spectral Granger causality to evaluate directed functional connectivity between 128 current sources (see Appendix 1 for details). We then performed 4 comparisons on the connectivity maps obtained from this analysis (Figure 1). To examine the emotion-induced networks, we identified functional connectivity in emotion-induced responses by evaluating changes in Granger causality going from RS to ES in the healthy control group (comparison 1) and in the MDD group (comparison 2).

To examine MDD-specific networks, we identified the effects of MDD on functional connectivity by evaluating differences in Granger causality between the MDD and healthy control groups during the RS (comparison 3) and ES (comparison 4) conditions. Furthermore, we theorized that different positive emotion responses between people with MDD and healthy controls may result from different interactions between latent subnetworks that are shared between the emotion-induced and MDD-specific networks. Therefore, we applied an unbiased data-driven decomposition approach to extract the shared latent components (or subnetworks) among the networks obtained from the 4 comparisons, and we evaluated the correlation between their activations across individual participants (Appendix 1).

### Comparison 1: emotion-induced functional connectivity in healthy controls

Figure 2A shows significant changes in Granger causality going from the RS to the ES in the healthy control group ( $\alpha = 0.05$ , 1000 permutations, false discovery rate [FDR] correction; see Appendix 1 for details). These connectivity changes are thought to contribute to the induced emotional response. We found increased connectivity over the frontal scalp; this was strongest in the  $\delta$  band (Figure 2A, top row). We also found decreased connectivity over the occipital and right temporal areas; this was strongest in the  $\alpha$  band (Figure 2A, bottom row). These networks can be further visualized by examining the sources and sinks of connectivity, which we quantified by summing all outgoing and incoming information flows at each channel. The sources and sinks of these networks are shown in Appendix 1, Figure S3.

**Table 1: Participant demographics and questionnaire data\***

Variable	Healthy controls <i>n</i> = 31	Participants with MDD† <i>n</i> = 24	<i>p</i> value	Effect size‡
Sex, female/male	17/14	15/9	0.57	0.063
Age, yr	29.74 ± 10.02	29.71 ± 10.93	0.99	0.003
Education, yr	16.94 ± 1.96	16.25 ± 2.56	0.22	0.303
Beck Depression Inventory II score	1.16 ± 2.02	24.96 ± 8.8	< 0.001**	3.728
Mood and Anxiety Symptoms Questionnaire§				
General Distress–Anxious Symptoms score	13.27 ± 2.02	21.29 ± 7.02	< 0.001**	1.553
Anxious Arousal score	17.67 ± 1.03	23.79 ± 8.33	< 0.005	1.031
General Distress–Depressive Symptoms score	13.67 ± 1.77	37.83 ± 10.36	< 0.001**	3.251
Anhedonic Depression score	44.97 ± 10.65	84.54 ± 10.39	< 0.001**	3.761
Ruminative Response Scale				
Depression subscale score	18.52 ± 4.70	32.54 ± 4.48	< 0.001**	3.054
Brooding subscale score	7.52 ± 2.03	12.63 ± 2.98	< 0.001**	2.004
Reflection subscale score	9.55 ± 3.57	12.13 ± 2.95	0.005	0.788
Pittsburgh Sleep Quality Index score¶	2.87 ± 1.93	8.48 ± 2.73	< 0.001**	2.373
Wechsler Test of Adult Reading score	118.03 ± 10.56	117.32 ± 7.76	0.79	0.077

MDD = major depressive disorder.

\*Values are mean ± standard deviation unless otherwise indicated. Statistics reflect between-group *t* tests except for sex ( $\chi^2$ ).

†Of the 24 participants with MDD, 2 met the criteria for generalized anxiety (past 6 months); 2 reported agoraphobia (past month); 2 reported social anxiety (past month); 2 reported panic attacks (last month); and 7 reported at least one panic attack (lifetime).

‡Cramer *V* for sex; otherwise Cohen *d*.

§Data were missing for 1 participant from the control group.

¶A score of 5 or less indicates good sleep quality; a score of greater than 5 indicates poor sleep quality.

\*\*Significant following Bonferroni correction for multiple comparisons.

### Comparison 2: emotion-induced functional connectivity in participants with MDD

Figure 2B shows significant changes in Granger causality going from the RS to the ES in the MDD group ( $\alpha = 0.05$ , 1000 permutations, FDR correction). As in the control group, we found increased connectivity in emotional response over the frontal scalp; this was strongest in the  $\delta$  band (Figure 2B, top row). However, in contrast to the results for the healthy control group, we found suppression of connectivity primarily over the parietal regions; this effect was again strongest in the  $\alpha$  band (Figure 2B, bottom row). The sources and sinks of these networks are shown in Appendix 1, Figure S4.

### Comparison 3: MDD-related functional connectivity during resting-state sessions

Figure 2C shows significant differences in Granger causality between the MDD and healthy control groups at rest ( $\alpha = 0.05$ , 1000 permutations, FDR correction). Compared to the control group, the MDD group showed stronger connectivity over the frontal area (primarily in the  $\delta$  band) and the parietal area (Figure 2C, top row), but weaker connectivity over the right temporal area (Figure 2C, bottom row). The sources and sinks of these networks are shown in Appendix 1, Figure S5.

### Comparison 4: MDD-related functional connectivity during emotion-induction sessions

Figure 2D shows significant differences in Granger causality between the MDD and healthy control groups during positive emotion induction ( $\alpha = 0.05$ , 1000 permutations, FDR correction). Compared to the healthy control group, the MDD group showed stronger connectivity scattered throughout the frontal area (primarily in the  $\delta$  band; Figure 2D, top row), and predominantly weaker connectivity spread out across the cortex (Figure 2D, bottom row). The sources and sinks of these networks are shown in Appendix 1, Figure S6.

### Extraction of principal subnetworks from all comparisons

To examine common subnetworks and obtain a comprehensive view of connectivity across all comparisons, we pooled significant connectivity from all comparisons to create a tensor with 3 dimensions (connection, frequency and comparison) and used an unbiased decomposition analysis (PARAFAC) to extract latent components in the functional networks shown in Figure 2 (see Appendix 1). We identified 2 dominant components — denoted subnetworks 1 and 2 — from the pooled connectivity (see factorization consistency in Appendix 1, Figure S7). Each component contained a unique fingerprint of network connections, spectral profiles and contributions to the 4 significant networks of the comparisons shown in Figure 2, described by its composition in the 3 tensor dimensions (Figure 3).

### Subnetwork 1: a task-positive $\delta$ -band frontal network

Spatially, subnetwork 1 consisted of strongly increased connectivity over the frontal cortex (Figure 3A, left) and weakly reduced connectivity over the right temporal cortex (Figure 3A, right; see source and sink areas in Appendix 1, Figure S8). Spectrally, subnetwork 1 appeared primarily in the  $\delta$  band (Figure 3B). Functionally, subnetwork 1 appeared strongly in the significant networks of comparison 1 (ES – RS in healthy controls) and comparison 2 (ES – RS in participants with MDD), and weakly in the significant networks of comparison 3 (RS in participants with MDD – RS in healthy controls) and comparison 4 (ES in participants with MDD – ES in healthy controls; Figure 3C, left). Based on this result, the activations of subnetwork 1 in each state of each participant group could be illustrated (Figure 3C, right). In summary, subnetwork 1 represented a  $\delta$ -band frontal network that was stronger in the ES than in the RS, indicating a task-positive network whose connectivity was enhanced during engagement with emotionally positive pictures. Activation of subnetwork 1 was stronger in the MDD group than the healthy control group at rest, but the increase in activity from rest to task (ES – RS) was greater in the healthy control group. This pattern suggests that, in the MDD group, subnetwork 1 was hyperactive at rest but hypoactive during emotion engagement.

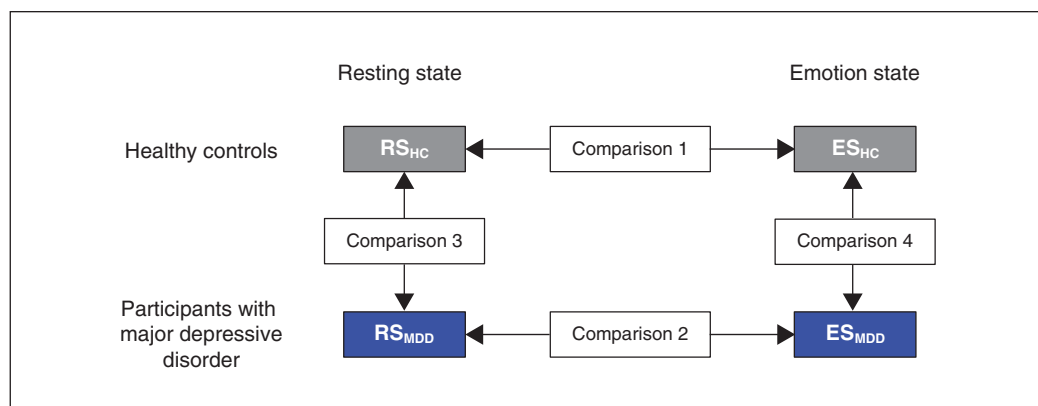


**Figure 1:** Four comparisons between states and participant groups. ES = emotion state; HC = healthy control; MDD = major depressive disorder; RS = resting state.

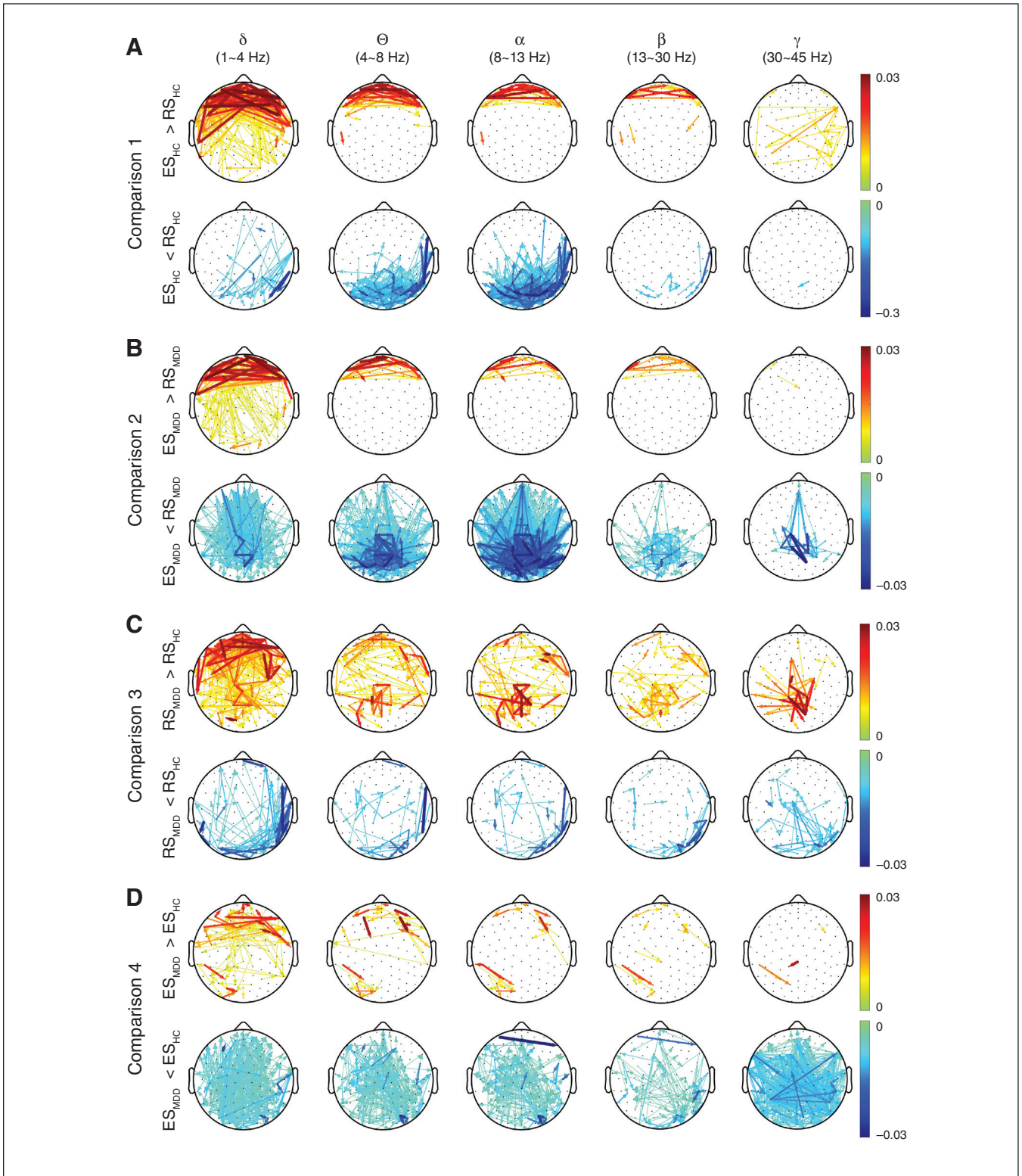


**Figure 2:** Significant networks from the 4 comparisons. Significant connections are shown for (A) comparison 1, (B) comparison 2, (C) comparison 3 and (D) comparison 4. For each significant connection, arrows represent the direction of information flow, and colour and thickness represent the size of the difference. For each comparison, positive differences are shown in the top row with a red colour scale (colour bar on the right), and negative differences are shown in the bottom row with a blue colour scale. ES = emotion state; HC = healthy control; MDD = major depressive disorder; RS = resting state.

### Subnetwork 2: a task-negative $\alpha$ -band parietal network

Subnetwork 2 consisted of increased connectivity over the parietal cortex (Figure 3D, left) with weakly reduced connectivity over the frontal cortex (Figure 3D, right; see source and sink areas in Appendix 1, Figure S8). This network appeared primarily in the  $\alpha$  band (Figure 3E). Furthermore, subnetwork 2 contributed negatively to the significant networks of comparison 1 (ES – RS in healthy controls), comparison 2 (ES – RS in participants with MDD) and comparison 4 (ES in participants with MDD – ES in healthy controls), but positively to the significant network of comparison 3 (RS in participants with MDD – RS in healthy controls; Figure 3F, left). We compiled this information to illustrate activity levels under different states and in both groups (Figure 3F, right). To summarize the significant findings, subnetwork 2 represented an  $\alpha$ -band parietal network that was less active in the ES than the RS, indicating a task-negative network that was suppressed during engagement with emotionally positive pictures. Furthermore, subnetwork 2 was more active in the MDD group than the healthy control group in the RS, but was less active in the MDD group than the healthy control group in the ES. This pattern suggests that subnetwork 2 was hyperactive at rest but strongly suppressed during task performance in the MDD group.

### Anticorrelation of subnetworks 1 and 2 during emotion induction

Relative to rest, subnetwork 1 connectivity was enhanced but subnetwork 2 connectivity was suppressed during positive emotion induction. To investigate further, we first evaluated how much subnetworks 1 and 2 contributed to emotion-induced responses in each participant. We achieved this by projecting the emotional response effect (ES – RS for healthy controls or participants with MDD) of each participant onto the spatio-spectral pattern (the first 2 dimensions) of each subnetwork (see Appendix 1). This method quantifies how much each subnetwork contributed to emotion-induced responses in each participant with a single scalar (i.e., the projection value).

The contributions of subnetworks 1 and 2 to emotion-induced responses for all participants are shown in Figure 4A and B. As expected, subnetwork 1 showed primarily positive contributions (task-positive) and subnetwork 2 showed primarily negative contributions (task-negative). We further plotted the activation levels of subnetwork 1 versus subnetwork 2 for each participant and evaluated their correlations in the healthy control and MDD groups (Figure 4C). We found significant correlations in both the healthy control group ( $R = -0.48, p = 0.006, R^2 = 0.23$ ) and the MDD group ( $R = -0.44, p = 0.033, R^2 = 0.19$ ), indicating anticorrelation between activity in these 2 networks. Furthermore, the sensitivities of this anticorrelation (regression slope) were  $-0.0142$  for

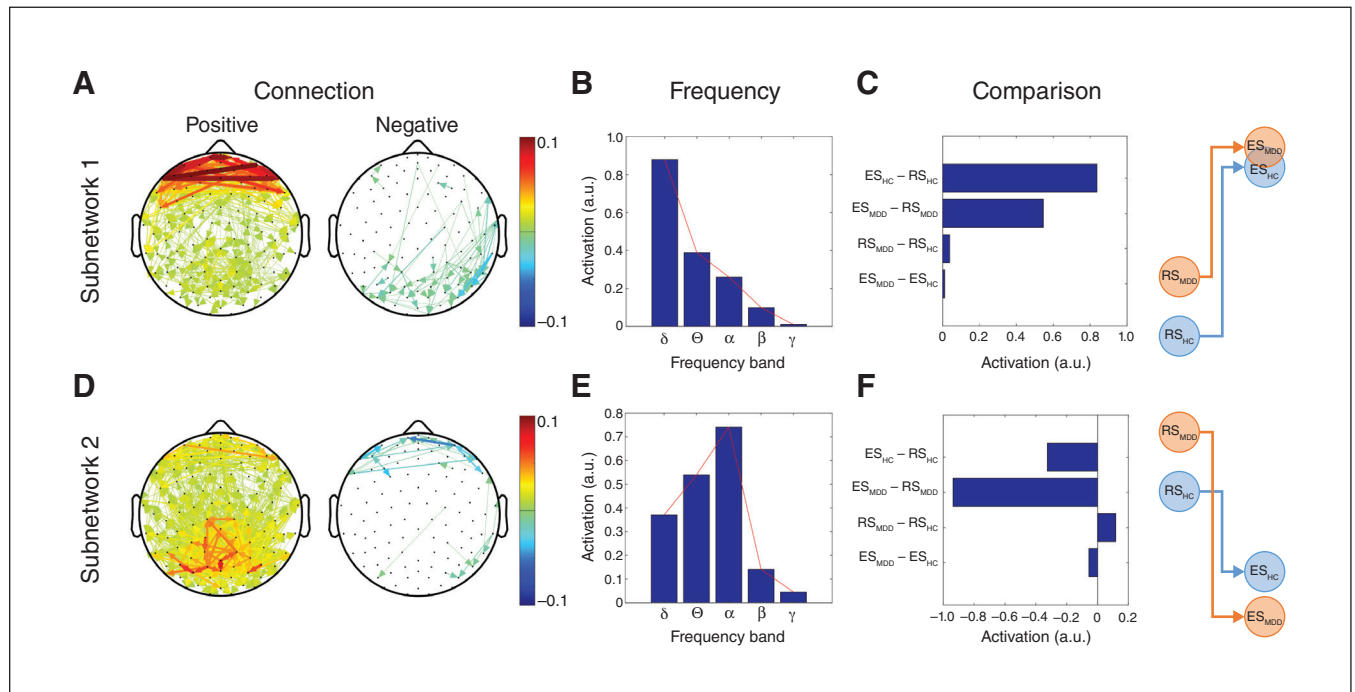


**Figure 3:** Subnetworks extracted from decomposition analysis (PARAFAC). (A) The spatial distribution of subnetwork 1. Positive connections are shown on the left, and negative connections are shown on the right. For each connection, arrows represent the direction of information flow, and colour and thickness represent the size of the difference. (B) The spectral distribution of subnetwork 1 in 5 different frequency bands. (C) The contribution of subnetwork 1 in the 4 comparisons is shown on the left, and can be used to illustrate the activations of subnetwork 1 in each state of each participant group (RS<sub>HC</sub>, ES<sub>HC</sub>, RS<sub>MDD</sub> and ES<sub>MDD</sub>) on the right. The contributions of subnetwork 2 in the same 3 dimensions are shown in (D), (E) and (F). ES = emotion state; HC = healthy control; MDD = major depressive disorder; RS = resting state.

the healthy control group and  $-0.0385$  for the MDD group, which were significantly different ( $p = 0.037$ ) by permutation test. We conducted the permutation test by comparing the difference in regression slopes ( $-0.0142$  and  $-0.0385$ ) to regression slopes recalculated from 5000 random shuffles of the group labels for each participant (as in Figure 4C). This finding indicated that, to achieve the same level of activation of subnetwork 1, more suppression of subnetwork 2 was required in people with MDD than in healthy controls.

#### Anticorrelation strength versus severity of depression symptoms

Finally, we examined whether the strength of anticorrelation in the MDD group (in the ES – RS contrast) was associated with depressive symptoms. For each participant with MDD, we measured the ratio of the activation levels between subnetwork 2 and subnetwork 1 (Figure 4D). A more negative ratio indicated that subnetwork 2 was more

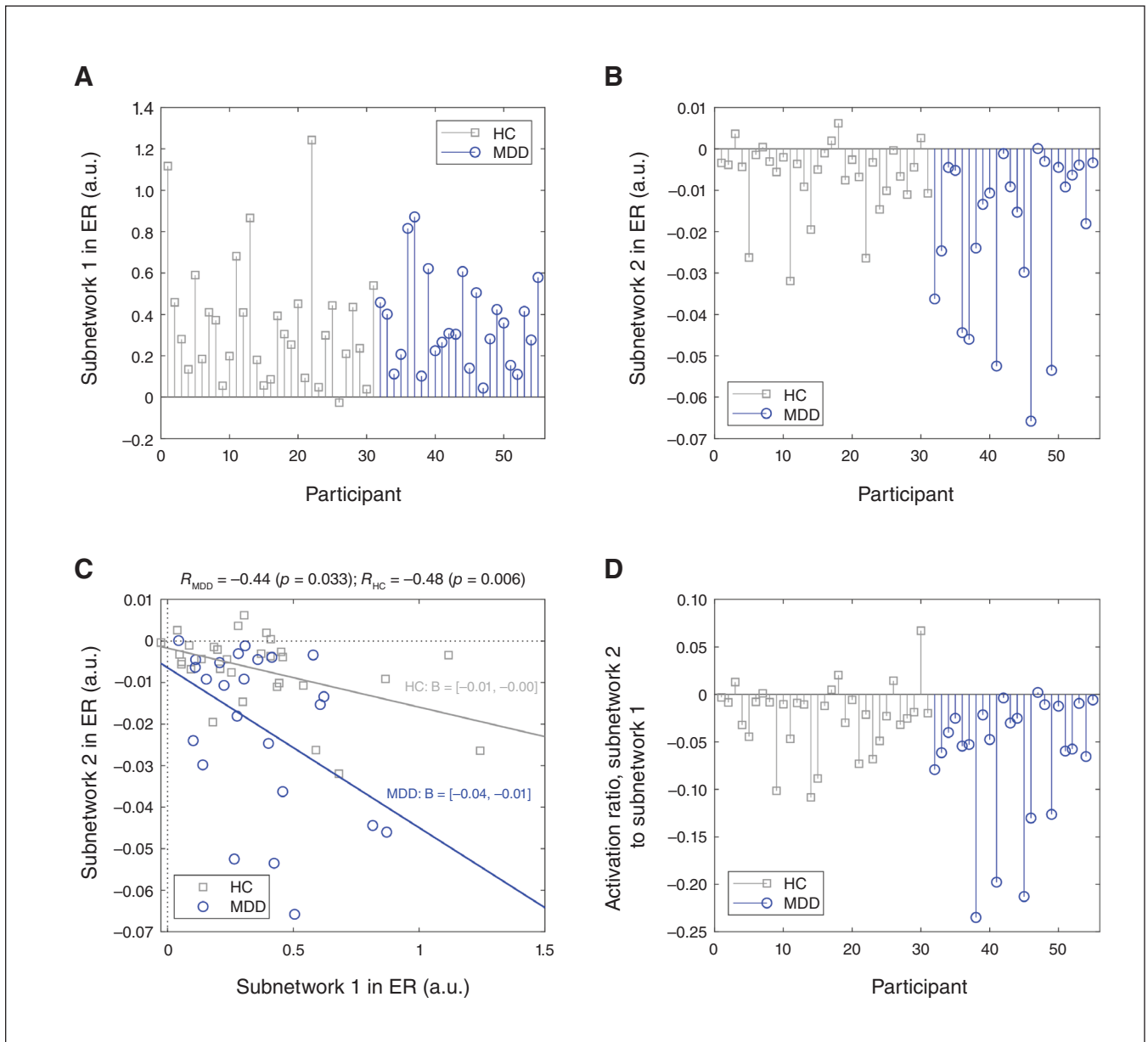


**Figure 4:** Activation of the subnetworks in emotion-induced responses in individuals. Healthy controls are shown with grey squares and participants with MDD are shown with blue circles. (A) Activation of subnetwork 1 in each participant. (B) Activation of subnetwork 2 in each participant. (C) Correlation between the activation levels of the 2 subnetworks. We performed linear regression analyses for participants with MDD and healthy controls; the correlation coefficients ( $R_{MDD}$  and  $R_{HC}$ ) and corresponding  $p$  values are shown. Regression results ( $B = [\text{slope}, \text{intercept}]$ ) are also shown. (D) The ratio of the activation level of subnetwork 2 to the activation level of subnetwork 1 for each participant. ER = emotional response; HC = healthy control; MDD = major depressive disorder.

strongly suppressed relative to the activation of subnetwork 1. We then plotted this ratio against the severity of depressive and anxious symptoms (because anxiety is commonly comorbid with MDD), as well as the level of trait rumination for each participant (Figure 5A). The Pearson correlation coefficients ( $R$ ) were as follows: Beck Depression Inventory II,  $-0.22$  ( $R^2 = 0.048$ ); MASQ Anhedonic Depression subscale,  $-0.49$  ( $R^2 = 0.24$ ); MASQ Anxious Arousal subscale,  $-0.04$  ( $R^2 = 0.0016$ ); MASQ General Distress–Depressive Symptoms subscale,  $-0.23$  ( $R^2 = 0.05$ ); MASQ General Distress–Anxious Symptoms subscale,  $-0.08$  ( $R^2 = 0.0064$ ); RSS Brooding subscale,  $-0.05$  ( $R^2 = 0.0025$ ); RSS Depression subscale,  $-0.44$  ( $R^2 = 0.19$ ); RSS Reflection subscale,  $-0.13$  ( $R^2 = 0.017$ ); and Pittsburgh Sleep Quality Index,  $-0.17$  ( $R^2 = 0.029$ ).

To evaluate the significance of these correlations, we randomly shuffled the symptom indices and recalculated the  $R$  values 10000 times, and then calculated the  $p$  value based on the distribution (Figure 5B; see Appendix 1). We found significant negative correlations for the MASQ anhedonic depression and RRS depression subscales ( $\alpha = 0.05$ , 10000 shuffles, FDR correction), suggesting that more suppression of subnetwork 2 was required during emotion engagement in patients with higher MASQ anhedonic depression and RRS depression scores. We found no correlations between symptom severity and activation of either subnetwork 1 or subnetwork 2 considered alone, or between symptom severity and the total energy required to activate both subnetworks (the sum of the absolute values of the activation levels of subnetworks 1 and 2; Appendix 1, Figure S9).

## Discussion

Depression is increasingly recognized as a network phenomenon, with excessive activation of task-negative networks (including the DMN) contributing to cardinal symptoms such as rumination.<sup>11</sup> The current study built on this previous work in 2 ways. First, by acquiring data during the resting-state but also during a positive emotion induction, we replicated network abnormalities at rest but also showed that such abnormalities contribute to abnormal positive emotional responses in adults with MDD. Specifically, we found that to mount the same task-positive response during the induction of positive emotion, more suppression of the task-negative networks is required for adults with MDD than for adults without depression. Second, by acquiring EEG rather than fMRI data, we were able to link depression to changes in networks with specific frequency profiles — namely, an  $\alpha$ -band parietal network and a  $\delta$ -band frontal network. This result was a useful contribution because oscillatory activity in different frequency bands has emerged as a fundamental mechanism of information processing and should facilitate translational work in nonhuman animals.<sup>47</sup> In the remainder of this discussion, we elaborate on these 2 points before considering limitations of the current work.

### *Two latent subnetworks revealed: a task-positive frontal $\delta$ network during induced emotion and a task-negative parietal $\alpha$ network during wakeful rest*

The first subnetwork is a task-positive network characterized by strong  $\delta$ -band functional connectivity over the frontal region; this network was more active during positive emotion induction than at rest. Potential sources of  $\delta$  oscillation have been found in both cortical (e.g., medial, middle and inferior frontal cortices, cingulate cortices) and subcortical regions (e.g., nucleus accumbens, ventral tegmental area), which are all directly or indirectly linked to reward and motivational processing.<sup>48–50</sup>

It has been argued that anhedonic MDD is closely linked to impaired reward processing and dysfunctional mesolimbic dopamine pathways.<sup>30,51</sup> In line with this proposal, we observed stronger frontal  $\delta$  connectivity (Figure 2C) and higher frontal  $\delta$  power in the MDD group than the healthy control group during the RS,<sup>52,53</sup> which seems to be associated with anhedonia,<sup>16</sup> melancholia<sup>15</sup> and somatic symptoms<sup>54</sup> of depression. Furthermore, our findings showed that, when engaging in positive emotion, the  $\delta$ -band connectivity change from the RS to the ES over the frontal area was reduced in the MDD group. Therefore, dysfunctional positive emotion in people with MDD could be characterized as a higher baseline (RS) frontal  $\delta$  connectivity or power but weaker connectivity change during exposure to emotionally positive material.

On the other hand, the task-negative parietal  $\alpha$  network we observed echoed some recent findings in which reduced resting-state EEG  $\alpha$ -band functional connectivity over the parietal–temporal region was correlated with greater anhedonia<sup>55</sup> or more severe symptoms.<sup>56</sup> Pretreatment  $\alpha$  power over posterior electrodes has also been linked to eventual treatment response.<sup>57,58</sup> We speculate that the large decrease of parietal  $\alpha$  connectivity from RS to ES that we observed in the MDD group may reflect reduced arousal and impaired processing of emotional stimuli,<sup>59,60</sup> which aligns with reduced mood reactivity in people with MDD.<sup>1</sup>

It is worth noting that the contribution in the  $\theta$  band was the second-highest for both subnetworks 1 and 2 (Figure 3B and E), suggesting its importance in both the task-positive and task-negative networks. Alteration of the  $\theta$  coherence in the frontal cortex<sup>53</sup> or along the frontocingulate axis<sup>61</sup> is indeed another commonly reported signature in people with MDD. Furthermore, increased pretreatment frontal  $\theta$  power appears to be a reliable predictor of treatment response to MDD.<sup>62,63</sup> Future treatment prediction studies might compare the predictive value of pretreatment  $\theta$  power alone versus combined with the pretreatment activation ratio between the 2 subnetworks identified here, which will be informative for guiding effective treatments.

### *Anhedonia and depressive rumination: extra suppression of the task-negative parietal network*

The task-positive frontal  $\delta$  network and the task-negative parietal  $\alpha$  network activated in an anticorrelated way:<sup>64</sup> the MDD group required more suppression of the task-negative network than the healthy control group to achieve comparable

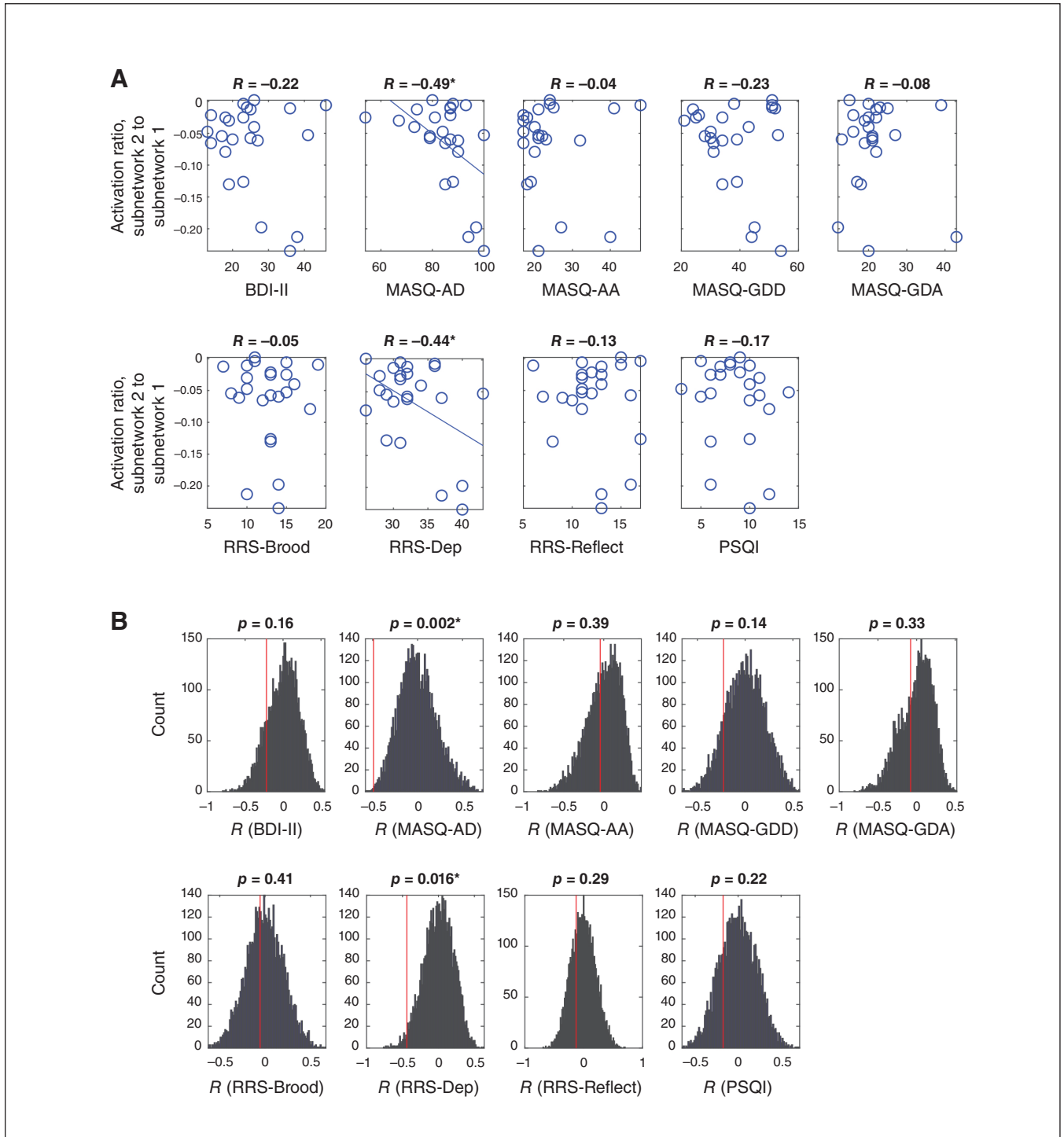


**Figure 5:** Anticorrelation sensitivity versus the severity of depression symptoms. (A) The ratio of the activation level of subnetwork 2 to the activation level of subnetwork 1 (shown in Figure 4D) is plotted against the severity of 9 symptoms related to MDD. Each circle represents the measurement from a participant with MDD. Pearson correlation coefficients ( $R$ ) are shown. Significant  $R$  values are indicated by an asterisk (see panel B), and the corresponding regression line is shown. (B) Significant  $R$  values identified by permutation. The distribution of the 10000  $R$  values from random shuffling is shown. The original  $R$  value is indicated as the red vertical line, and the corresponding  $p$  value is shown. Significant values are indicated by an asterisk ( $\alpha = 0.05$ , 10000 shuffles, FDR correction). AA = Anxious Arousal; AD = Anhedonic Depression; BDI-II = Beck Depression Inventory II; Brood = brooding subscale; Dep = depression subscale; FDR = false discovery rate; GDA = General Distress–Anxious Symptoms; GDD = General Distress–Depressive Symptoms; MASQ = Mood and Anxiety Symptoms Questionnaire; MDD = major depressive disorder; PSQI = Pittsburgh Sleep Quality Index; Reflect = reflection subscale; RRS = Ruminative Response Scale.

activation in the task-positive network. Furthermore, we showed that abnormal anticorrelation of task-positive and task-negative networks could contribute to anhedonia (reduced pleasure) and depressive rumination (negative thinking loops) — 2 core symptoms of MDD. This result supports the hypothesis that the overshadowing of task-positive networks by task-negative networks during emotion engagement may contribute to MDD.<sup>23,65</sup> First, for people with a higher tendency toward depressive rumination, the task-negative subnetwork is usually overactive at rest, possibly reflecting depressive rumination.<sup>52,54,65,66</sup> Second, deficient suppression of the task-negative subnetwork may make it difficult for people with MDD to disengage the overactive task-negative subnetwork, which may support maladaptive rumination.<sup>23</sup> Consequently, when faced with positive events or contexts, adults with depression may need to expend more energy to suppress the overactive task-negative network in order to fully engage in positive emotion. The need to expend extra effort could be one reason why it is more difficult for depressed adults to experience pleasure in response to positive events.

#### *Potential clinical utility of the ratio of task-negative to task-positive activation*

If the current findings can be replicated, they may have clinical utility. First, the ratio of task-negative to task-positive activation — or the ratio of parietal  $\alpha$  subnetwork to frontal  $\delta$  subnetwork activation — could be of use when assessing the severity of MDD. Many EEG studies,<sup>67</sup> including some of ours,<sup>37,38,68</sup> have shown the power of EEG features for MDD detection. Furthermore, one of our previous studies (using the same data set as the current study) showed that the classification performance of EEG features extracted during an emotion-induction state was better than those extracted from the resting state.<sup>37</sup> However, most of these studies focused mainly on searching for discriminative features that perform well in binary classification problems. In contrast, the ratio of task-positive to task-negative ratio activation highlighted here, which was correlated with levels of anhedonia and depressive rumination, could be applied to evaluate the severity of depression. Second, the anticorrelation of the 2 subnetworks also raises the possibility of new treatment targets for neuromodulatory approaches, such as transcranial magnetic stimulation (TMS) or transcranial direct or alternating current stimulation.

Over the past 2 decades, repetitive TMS (rTMS) has been widely applied over the frontal region to treat MDD,<sup>69</sup> and it seems to work by reducing hyperconnectivity in the DMN while regaining the anticorrelation between the DMN and other subnetworks.<sup>70</sup> Our results suggest that, in addition to frontal regions, modulating the parietal  $\alpha$  subnetwork could be another target for TMS-based treatment. For example, both rTMS and transcranial alternating current stimulation<sup>71</sup> could be applied to normalize the  $\alpha$  rhythm over the parietal area and achieve more efficient suppression of the task-negative parietal  $\alpha$  network.

#### *Limitations*

Several limitations should be noted. First, our sample size was not large, which may raise concerns about generalizability. To compensate for this limitation, we took a non-parametric resampling approach with FDR correction to test the statistical significance of the connectivity contrast analyses and correlation analyses. However, given the heterogeneous nature of MDD, it remains to be verified whether the observed effect was specific to this MDD sample or could be generalized to others. Second, DMN dysfunction has also been reported in other mental disorders (e.g., schizophrenia, anxiety, autism spectrum disorder),<sup>72</sup> so the anticorrelation of the 2 subnetworks may not be specific to MDD. Studies with larger samples and better representation of commonly comorbid disorders (e.g., generalized anxiety disorder) are needed to test the generalizability of the current findings and examine whether there are sex differences. Third, in addition to the reduced ability to feel pleasure, people with depression frequently show excessive negative emotions and difficulty disengaging from negative stimuli.<sup>6,73</sup> Future studies using both negative and positive stimuli will be needed to examine the role of the task-positive frontal  $\delta$  networks in negative emotion. Last but not least, the limited spatial resolution of EEG prohibits strong conclusions about functional anatomy. Although the interpretations made here are supported by previous EEG and fMRI studies, future studies using a multimodal neuroimaging approach (e.g., simultaneous EEG and fMRI) are needed to provide further convergent evidence regarding the source of the 2 subnetworks.

#### **Conclusion**

Our work shows that altered coordination between a task-positive frontal  $\delta$  network and a task-negative parietal  $\alpha$  network contributes to impaired positive emotional responses, anhedonia and depressive rumination in unmedicated adults with MDD. These findings provide new insight into the pathophysiology of depression and highlight targets for treatment with noninvasive brain stimulation in future work.

**Affiliations:** From the International Research Center for Neurointelligence (WPI-IRCN), UTIAS, The University of Tokyo, Tokyo, Japan (Chao, Wu); the Center for Depression, Anxiety and Stress Research, McLean Hospital, Belmont, Mass. (Dillon, Barrick); Harvard Medical School, Boston, Mass. (Dillon); the Department of Mechanical Engineering, National Taiwan University of Science and Technology, Taiwan (Liu); the Yuan-Rung Medical System, Changhua, Taiwan (Liu).

**Funding:** Data collection for this project was supported by funding from McLean Hospital provided to D. Dillon. D. Dillon and E. Barrick were supported by National Institutes of Mental Health (NIMH) grant R00MH094438, awarded to D. Dillon. D. Dillon was also supported by NIMH grant R01MH111676. C. Wu was supported by the Ministry of Science and Technology of Taiwan (MOST 105-2314-B-002-029- and MOST 106-2420-H-002-008-MY2, awarded to C. Wu). This work was supported by the World Premier International Research Center Initiative, MEXT, Japan.

**Competing interests:** None declared.

**Contributors:** Z. Chao and C. Wu designed the study. D. Dillon, Y. Liu and E. Barrick acquired the data, which Z. Chao, D. Dillon and C. Wu analyzed. Z. Chao, D. Dillon and C. Wu wrote the article, which D. Dillon, Y. Liu, E. Barrick and C. Wu reviewed. All authors approved the final version to be published, agree to be accountable for all aspects of the work and can certify that no other individuals not listed as authors have made substantial contributions to the paper.

**Content licence:** This is an Open Access article distributed in accordance with the terms of the Creative Commons Attribution (CC BY-NC-ND 4.0) licence, which permits use, distribution and reproduction in any medium, provided that the original publication is properly cited, the use is noncommercial (i.e., research or educational use), and no modifications or adaptations are made. See: <https://creativecommons.org/licenses/by-nc-nd/4.0/>

## References

- American Psychiatric Association. *Diagnostic and statistical manual of mental disorders*. Fifth edition. Arlington (VA): American Psychiatric Association Publishing; 2013.
- Proudman D, Greenberg P, Nellesen D. The growing burden of major depressive disorders (MDD): implications for researchers and policy makers. *Pharmacoeconomics* 2021;39:619-25.
- Boku S, Nakagawa S, Toda H, et al. Neural basis of major depressive disorder: beyond monoamine hypothesis: neural basis of major depressive disorder. *Psychiatry Clin Neurosci* 2018;72:3-12.
- Hirschfeld RMA. History and evolution of the monoamine hypothesis of depression. *J Clin Psychiatry* 2000;61:4-6.
- Konjedi S, Maleeh R. A closer look at the relationship between the default network, mind wandering, negative mood, and depression. *Cogn Affect Behav Neurosci* 2017;17:697-711.
- Koster EHW, De Lissnyder E, Derakshan N, et al. Understanding depressive rumination from a cognitive science perspective: the impaired disengagement hypothesis. *Clin Psychol Rev* 2011;31:138-45.
- Park C, Rosenblat JD, Lee Y, et al. The neural systems of emotion regulation and abnormalities in major depressive disorder. *Behav Brain Res* 2019;367:181-8.
- Post RJ, Warden MR. Melancholy, anhedonia, apathy: the search for separable behaviors and neural circuits in depression. *Curr Opin Neurobiol* 2018;49:192-200.
- Hamilton JP, Farmer M, Fogelman P, et al. Depressive rumination, the default-mode network, and the dark matter of clinical neuroscience. *Biol Psychiatry* 2015;78:224-30.
- Kaiser RH, Andrews-Hanna JR, Wager TD, et al. Large-scale network dysfunction in major depressive disorder: a meta-analysis of resting-state functional connectivity. *JAMA Psychiatry* 2015;72:603-11.
- Berman MG, Peltier S, Nee DE, et al. Depression, rumination and the default network. *Soc Cogn Affect Neurosci* 2011;6:548-55.
- Miller CH, Hamilton JP, Sacchet MD, et al. Meta-analysis of functional neuroimaging of major depressive disorder in youth. *JAMA Psychiatry* 2015;72:1045.
- Zhu X, Wang X, Xiao J, et al. Evidence of a dissociation pattern in resting-state default mode network connectivity in first-episode, treatment-naive major depression patients. *Biol Psychiatry* 2012;71:611-7.
- Neuner I, Arrubla J, Werner CJ, et al. The default mode network and EEG regional spectral power: a simultaneous fMRI-EEG study. *PLoS ONE* 2014;9:e88214.
- Pizzagalli DA, Oakes TR, Fox AS, et al. Functional but not structural subgenual prefrontal cortex abnormalities in melancholia. *Mol Psychiatry* 2004;9:325-405.
- Wacker J, Dillon DG, Pizzagalli DA. The role of the nucleus accumbens and rostral anterior cingulate cortex in anhedonia: integration of resting EEG, fMRI, and volumetric techniques. *Neuroimage* 2009;46:327-37.
- Borserio BJ, Sharpley CF, Bitsika V, et al. Default mode network activity in depression subtypes. *Rev Neurosci* 2021;32:597-613.
- Drysdale AT, Grosenick L, Downar J, et al. Resting-state connectivity biomarkers define neurophysiological subtypes of depression. *Nat Med* 2017;23:28-38.
- Sharpley CF, Bitsika V. Validity, reliability and prevalence of four "clinical content" subtypes of depression. *Behav Brain Res* 2014;259:9-15.
- Mayberg HS, Lozano AM, Voon V, et al. Deep brain stimulation for treatment-resistant depression. *Neuron* 2005;45:651-60.
- Chin Fatt CR, Jha MK, Cooper CM, et al. Effect of intrinsic patterns of functional brain connectivity in moderating antidepressant treatment response in major depression. *Am J Psychiatry* 2020;177:143-54.
- Nejad AB, Fossati P, Lemogne C. Self-referential processing, rumination, and cortical midline structures in major depression. *Front Hum Neurosci* 2013;7:666.
- Pizzagalli DA. Frontocingulate dysfunction in depression: toward biomarkers of treatment response. *Neuropsychopharmacology* 2011;36:183-206.
- Preuss A, Bolliger B, Schicho W, et al. SSRI treatment response prediction in depression based on brain activation by emotional stimuli. *Front Psychiatry* 2020;11:538393.
- Spies M, Kraus C, Geissberger N, et al. Default mode network deactivation during emotion processing predicts early antidepressant response. *Transl Psychiatry* 2017;7:e1008.
- Guha A, Yee CM, Heller W, et al. Alterations in the default mode-salience network circuit provide a potential mechanism supporting negativity bias in depression. *Psychophysiology* 2021;58:e13918.
- Ho TC, Connolly CG, Henje Blom E, et al. Emotion-dependent functional connectivity of the default mode network in adolescent depression. *Biol Psychiatry* 2015;78:635-46.
- Sheline YI, Barch DM, Price JL, et al. The default mode network and self-referential processes in depression. *Proc Natl Acad Sci U S A* 2009;106:1942-7.
- Zhang B, Li S, Zhuo C, et al. Altered task-specific deactivation in the default mode network depends on valence in patients with major depressive disorder. *J Affect Disord* 2017;207:377-83.
- Pizzagalli DA. Depression, stress, and anhedonia: toward a synthesis and integrated model. *Annu Rev Clin Psychol* 2014;10:393-423.
- Pizzagalli DA. Toward a better understanding of the mechanisms and pathophysiology of anhedonia: are we ready for translation? *Am J Psychiatry* 2022;179:458-69.
- Chao ZC, Sawada M, Isa T, et al. Dynamic reorganization of motor networks during recovery from partial spinal cord injury in monkeys. *Cerebral Cortex* 2019;29:3059-73.
- Chao ZC, Takaura K, Wang L, et al. Large-scale cortical networks for hierarchical prediction and prediction error in the primate brain. *Neuron* 2018;100:1252-66.e3.
- Chao ZC, Nagasaka Y, Fujii N. Cortical network architecture for context processing in primate brain. *eLife* 2015;4:e06121.
- Beck AT, Steer RA, Brown GK. *Manual for the Beck Depression Inventory-II*. San Antonio (TX): Psychological Corporation; 1996.
- Sheehan DV, Lecrubier Y, Sheehan KH, et al. The Mini-International Neuropsychiatric Interview (M.I.N.I.): the development and validation of a structured diagnostic psychiatric interview for DSM-IV and ICD-10. *J Clin Psychiatry* 1998;59(Suppl. 20):22-33.
- Wu C-T, Dillon D, Hsu H-C, et al. Depression detection using relative EEG power induced by emotionally positive images and a conformal kernel support vector machine. *Appl Sci (Basel)* 2018;8:1244.
- Liao S-C, Wu C-T, Huang H-C, et al. Major depression detection from EEG signals using kernel eigen-filter-bank common spatial patterns. *Sensors (Basel)* 2017;17:1385.
- Peirce JW. PsychoPy—psychophysics software in Python. *J Neurosci Methods* 2007;162:8-13.
- Dillon DG, Pizzagalli DA. Evidence of successful modulation of brain activation and subjective experience during reappraisal of negative emotion in unmedicated depression. *Psychiatry Res* 2013;212:99-107.
- Bradley MM, Lang PJ. Measuring emotion: the self-assessment manikin and the semantic differential. *J Behav Ther Exp Psychiatry* 1994;25:49-59.
- Lang PJ, Bradley MM, Cuthbert BN. *International Affective Picture System (IAPS): Affective ratings of pictures and instruction manual; technical report A-8*. Gainesville (FL): University of Florida; 2008.

43. Watson D, Weber K, Assenheimer JS, et al. Testing a tripartite model: I. Evaluating the convergent and discriminant validity of anxiety and depression symptom scales. *J Abnorm Psychol* 1995;104:3-14.
44. Treynor W, Gonzalez R, Nolen-Hoeksema S. Rumination reconsidered: a psychometric analysis. *Cognit Ther Res* 2003;27:247-259.
45. Buysse DJ, Reynolds CF, Monk TH, et al. The Pittsburgh Sleep Quality Index: a new instrument for psychiatric practice and research. *Psychiatry Res* 1989;28:193-213.
46. Miljevic A, Bailey NW, Vila-Rodriguez F, et al. Electroencephalographic connectivity: a fundamental guide and checklist for optimal study design and evaluation. *Biol Psychiatry Cogn Neurosci Neuroimaging* 2022;7:546-54.
47. Buzsáki G, Draguhn A. Neuronal oscillations in cortical networks. *Science* 2004;304:1926-9.
48. Harmony T. The functional significance of delta oscillations in cognitive processing. *Front Integr Neurosci* 2013;7:83.
49. Knyazev GG. Motivation, emotion, and their inhibitory control mirrored in brain oscillations. *Neurosci Biobehav Rev* 2007;31:377-95.
50. Knyazev GG. EEG delta oscillations as a correlate of basic homeostatic and motivational processes. *Neurosci Biobehav Rev* 2012;36:677-95.
51. Treadway MT, Zald DH. Reconsidering anhedonia in depression: lessons from translational neuroscience. *Neurosci Biobehav Rev* 2011;35:537-55.
52. Knyazev GG, Savostyanov AN, Bocharov AV, et al. Task-positive and task-negative networks in major depressive disorder: a combined fMRI and EEG study. *J Affect Disord* 2018;235:211-9.
53. McVoy M, Aebi ME, Loparo K, et al. Resting-state quantitative electroencephalography demonstrates differential connectivity in adolescents with major depressive disorder. *J Child Adolesc Psychopharmacol* 2019;29:370-7.
54. Knyazev GG, Savostyanov AN, Bocharov AV, et al. Task-positive and task-negative networks and their relation to depression: EEG beamformer analysis. *Behav Brain Res* 2016;306:160-9.
55. Rolle CE, Fonzo GA, Wu W, et al. Cortical connectivity moderators of antidepressant vs placebo treatment response in major depressive disorder: secondary analysis of a randomized clinical trial. *JAMA Psychiatry* 2020;77:397.
56. Mohammadi Y, Moradi MH. Prediction of depression severity scores based on functional connectivity and complexity of the EEG signal. *Clin EEG Neurosci* 2021;52:52-60.
57. Bruder GE, Sedoruk JP, Stewart JW, et al. Electroencephalographic alpha measures predict therapeutic response to a selective serotonin reuptake inhibitor antidepressant: pre- and post-treatment findings. *Biol Psychiatry* 2008;63:1171-7.
58. Tenke CE, Kayser J, Manna CG, et al. Current source density measures of electroencephalographic alpha predict antidepressant treatment response. *Biol Psychiatry* 2011;70:388-94.
59. Bruder GE, Stewart JW, McGrath PJ. Right brain, left brain in depressive disorders: clinical and theoretical implications of behavioral, electrophysiological and neuroimaging findings. *Neurosci Biobehav Rev* 2017;78:178-91.
60. Heller W, Nitschke JB. Regional brain activity in emotion: a framework for understanding cognition in depression. *Cogn Emotion* 1997;11:637-61.
61. Pizzagalli DA, Oakes TR, Davidson RJ. Coupling of theta activity and glucose metabolism in the human rostral anterior cingulate cortex: an EEG/PET study of normal and depressed subjects. *Psychophysiology* 2003;40:939-49.
62. Korb AS, Hunter AM, Cook IA, et al. Rostral anterior cingulate cortex theta current density and response to antidepressants and placebo in major depression. *Clin Neurophysiol* 2009;120:1313-9.
63. Pizzagalli DA, Webb CA, Dillon DG, et al. Pretreatment rostral anterior cingulate cortex theta activity in relation to symptom improvement in depression: a randomized clinical trial. *JAMA Psychiatry* 2018;75:547.
64. Fox MD, Snyder AZ, Vincent JL, et al. The human brain is intrinsically organized into dynamic, anticorrelated functional networks. *Proc Natl Acad Sci U S A* 2005;102:9673-8.
65. Marchetti I, Koster EHW, Sonuga-Barke EJ, et al. The default mode network and recurrent depression: a neurobiological model of cognitive risk factors. *Neuropsychol Rev* 2012;22:229-51.
66. Hamilton JP, Furman DJ, Chang C, et al. Default-mode and task-positive network activity in major depressive disorder: implications for adaptive and maladaptive rumination. *Biol Psychiatry* 2011;70:327-33.
67. Cukic M, López V, Pavón J. Classification of depression through resting-state electroencephalogram as a novel practice in psychiatry. *J Med Internet Res* 2020;22:e19548.
68. Wu C-T, Huang H-C, Huang S, et al. Resting-state EEG signal for major depressive disorder detection: a systematic validation on a large and diverse dataset. *Biosensors (Basel)* 2021;11:499.
69. Schutter DJLG. Antidepressant efficacy of high-frequency transcranial magnetic stimulation over the left dorsolateral prefrontal cortex in double-blind sham-controlled designs: a meta-analysis. *Psychol Med* 2009;39:65-75.
70. Liston C, Chen AC, Zebley BD, et al. Default mode network mechanisms of transcranial magnetic stimulation in depression. *Biol Psychiatry* 2014;76:517-26.
71. Hosseinian T, Yavari F, Biagi MC, et al. External induction and stabilization of brain oscillations in the human. *Brain Stimul* 2021;14:579-87.
72. Broyd SJ, Demanuele C, Debener S, et al. Default-mode brain dysfunction in mental disorders: a systematic review. *Neurosci Biobehav Rev* 2009;33:279-96.
73. Disner SG, Beevers CG, Haigh EAP, et al. Neural mechanisms of the cognitive model of depression. *Nat Rev Neurosci* 2011;12:467-77.